

# Ecosystem modeling of methane and carbon dioxide fluxes for boreal forest sites

Christopher Potter, Jill Bubier, Patrick Crill, and Peter Lafleur

**Abstract:** Predicted daily fluxes from an ecosystem model for water, carbon dioxide, and methane were compared with 1994 and 1996 Boreal Ecosystem–Atmosphere Study (BOREAS) field measurements at sites dominated by old black spruce (*Picea mariana* (Mill.) BSP) (OBS) and boreal fen vegetation near Thompson, Man. Model settings for simulating daily changes in water table depth (WTD) for both sites were designed to match observed water levels, including predictions for two microtopographic positions (hollow and hummock) within the fen study area. Water run-on to the soil profile from neighboring microtopographic units was calibrated on the basis of daily snowmelt and rainfall inputs to reproduce BOREAS site measurements for timing and magnitude of maximum daily WTD for the growing season. Model predictions for daily evapotranspiration rates closely track measured fluxes for stand water loss in patterns consistent with strong controls over latent heat fluxes by soil temperature during nongrowing season months and by variability in relative humidity and air temperature during the growing season. Predicted annual net primary production (NPP) for the OBS site was 158 g C·m<sup>-2</sup> during 1994 and 135 g C·m<sup>-2</sup> during 1996, with contributions of 75% from overstory canopy production and 25% from ground cover production. Annual NPP for the wetter fen site was 250 g C·m<sup>-2</sup> during 1994 and 270 g C·m<sup>-2</sup> during 1996. Predicted seasonal patterns for soil CO<sub>2</sub> fluxes and net ecosystem production of carbon both match daily average estimates at the two sites. Model results for methane flux, which also closely match average measured flux levels of -0.5 mg CH<sub>4</sub>·m<sup>-2</sup>·day<sup>-1</sup> for OBS and 2.8 mg CH<sub>4</sub>·m<sup>-2</sup>·day<sup>-1</sup> for fen sites, suggest that spruce areas are net annual sinks of about -0.12 g CH<sub>4</sub>·m<sup>-2</sup>, whereas fen areas generate net annual emissions on the order of 0.3–0.85 g CH<sub>4</sub>·m<sup>-2</sup>, depending mainly on seasonal WTD and microtopographic position. Fen hollow areas are predicted to emit almost three times more methane during a given year than fen hummock areas. The validated model is structured for extrapolation to regional simulations of interannual trace gas fluxes over the entire North America boreal forest, with integration of satellite data to characterize properties of the land surface.

**Résumé :** Les flux quotidiens prédits par un modèle écosystémique pour l'eau, le dioxyde de carbone et le méthane ont été comparés aux mesures prises sur le terrain en 1994 et 1996 dans le cadre de l'étude de l'atmosphère et de l'écosystème boréal (BOREAS) dans des sites dominés soit par un vieux peuplement d'épinette noire (*Picea mariana* (Mill.) BSP), soit par une végétation de fen boréal et situés près de Thompson, au Manitoba. Les paramètres du modèle utilisé pour simuler les variations quotidiennes de la profondeur de la nappe phréatique pour les deux sites ont été ajustés pour correspondre aux niveaux d'eau observés, incluant les prévisions pour deux positions micro-topographiques (dépressions et hummocks) dans la zone d'étude de trouvant dans le fen. L'arrivée d'eau dans le profil de sol en provenance des unités micro-topographiques avoisinantes a été calibrée sur la base des apports quotidiens dus à la pluie ou à la fonte de la neige, afin de reproduire les mesures prises sur le site de BOREAS concernant le moment et l'ampleur de la profondeur quotidienne maximale de la nappe phréatique pendant la saison de croissance. Les prédictions du modèle pour le taux quotidien d'évapotranspiration suivent de très près les flux mesurés de perte d'eau du peuplement dont le comportement est consistant avec de forts contrôles sur les flux de chaleur latente par la température du sol durant les mois de dormance et par la variabilité de l'humidité relative et de la température de l'air pendant la saison de croissance. Dans le site dominé par l'épinette noire, le modèle a prédit une production primaire nette annuelle de 158 g C·m<sup>-2</sup> en 1994 et de 135 g C·m<sup>-2</sup> en 1996 qui provient dans des proportions de 75% du couvert de l'étage dominant et de 25% de la végétation au sol. La production primaire nette annuelle dans le site plus humide de fen atteignait respectivement 250 et 270 g C·m<sup>-2</sup> en 1994 et 1996. Les patrons saisonniers prédits par le modèle pour les flux de CO<sub>2</sub> dans le sol et la production nette de carbone par l'écosystème étaient comparables aux estimés de la moyenne journalière dans les deux sites. Les résultats du modèle pour le flux de méthane, qui sont très près des niveaux moyens qui ont été mesurés soit -0,5 mg CH<sub>4</sub>·m<sup>-2</sup>·jour<sup>-1</sup> pour le site dominé par l'épinette et 2,8 mg CH<sub>4</sub>·m<sup>-2</sup>·jour<sup>-1</sup> pour le fen, suggèrent que les zones occupées par l'épinette noire sont des puits avec une valeur annuelle nette de -0,12 g CH<sub>4</sub>·m<sup>-2</sup>, tandis que les zones occupées par le fen génèrent des émissions annuelles nettes de l'ordre de 0,3 à 0,85 g CH<sub>4</sub>·m<sup>-2</sup>,

Received April 10, 2000. Accepted November 8, 2000. Published on the NRC Research Press website on February 2, 2001.

**C. Potter.**<sup>1</sup> NASA, Ames Research Center, Ecosystem Science and Technology Branch, Moffett Field, CA 94035, U.S.A.

**J. Bubier.** Mount Holyoke College, South Hadley, MA 01075, U.S.A.

**P. Crill.** University of New Hampshire, Durham, NH 03824, U.S.A.

**P. Lafleur.** Trent University, Peterborough, ON K9J 7B8, Canada.

<sup>1</sup>Corresponding author. e-mail: cpotter@gaia.arc.nasa.gov

qui varient surtout en fonction de la profondeur saisonnière de la nappe phréatique et de la position micro-topographique. Selon les prédictions, les zones de dépression émettraient presque trois fois plus de méthane au cours d'une année que les zones de hummock dans le fen. Le modèle qui a été validé est structuré pour extrapoler à l'échelle régionale les flux inter-annuels de gaz traces pour l'ensemble de la forêt boréale en Amérique du Nord, avec l'intégration de données satellitaires pour caractériser les propriétés de la surface du territoire.

## Introduction

The Boreal Ecosystem–Atmosphere Study (BOREAS) project has addressed several fundamental questions concerning moisture and carbon (C) in the boreal forest biome (Hall et al. 1996). These questions include what are the primary mechanisms controlling variability in water and carbon fluxes within each of the major boreal ecosystem types, and what measured parameters are most important in terms of scaling up the seasonal patterns of water and carbon cycling across diverse ecosystem types within the boreal forest region? Measurement of net ecosystem exchange of carbon at BOREAS sites may clarify issues concerning the proposed northern hemisphere boreal carbon sink.

As is the case with carbon dioxide fluxes, wetland emissions of methane (CH<sub>4</sub>) are closely tied to thermal fluxes and hydrologic cycles in boreal ecosystems. Consequently, methane has been a trace gas of special interest in the BOREAS (BOREAS Science Team 1995; Bubier et al. 1995a; Sellers et al. 1995; Hall et al. 1996; Suyker et al. 1996). Methane is a greenhouse gas with 4–35 times the global warming potential of carbon dioxide on a molar basis (Houghton et al. 1992). Approximately 110 Tg CH<sub>4</sub> (1 Tg = 10<sup>12</sup> g) is emitted from natural wetland sources worldwide, which is equivalent to 20% of the methane entering the atmosphere each year (Cicerone and Oremland 1988; Fung et al. 1991). The global boreal forest could contribute nearly 19 Tg CH<sub>4</sub> per year to the atmosphere (Bartlett and Harriss 1993; Bachand et al. 1996).

Fluxes of CO<sub>2</sub> and CH<sub>4</sub> have been measured previously at a relatively small number of locations in the North America boreal forest (Roulet et al. 1992a; Bartlett and Harriss 1993; Bubier et al. 1995a; Moosavi and Crill 1997). However, construction of an accurate regional emission budget for any biogenic trace gas from a relatively limited data set of measurements carries a high degree of uncertainty. Variability in emission rates from year to year and among ecosystem types can be high, a fact that makes generalizations difficult to substantiate in the course of extrapolation of fluxes to a region. Use of a process-oriented simulation model that includes major gas flux controllers can facilitate interpretation of gas flux estimates along regional transects of interest and assist in generation of regionwide model estimates of seasonal flux budgets, which may be verified using independent site measurements.

Previous studies of ecosystem carbon cycling and trace gas biogeochemistry for the BOREAS region (e.g., Bonan 1991; Bubier et al. 1995a, 1995b; Frolking et al. 1996; Moosavi and Crill 1997; Goulden et al. 1998) have demonstrated the importance of describing several ecosystem components as part of simulation modeling for soil respiration and methane fluxes: (i) differentiation of effects of understory and ground cover vegetation (such as the moss layer in spruce stands) on surface moisture, temperature, and net production estimates in boreal forests; (ii) distribution of per-

mafrost as it relates to thermal and water table controls on carbon mineralization rates; (iii) plant community composition as it relates to labile carbon and nutrient sources, such as root exudates, and emission pathways for trace gases through plant tissues; (iv) wetland microtopographic (i.e., hummocks and hollows) effects on the same variables listed in the first two observations above; and (v) properties of transition zones from (wetland to upland) as areas of rapid changes in thermal and water table controls on biogeochemistry.

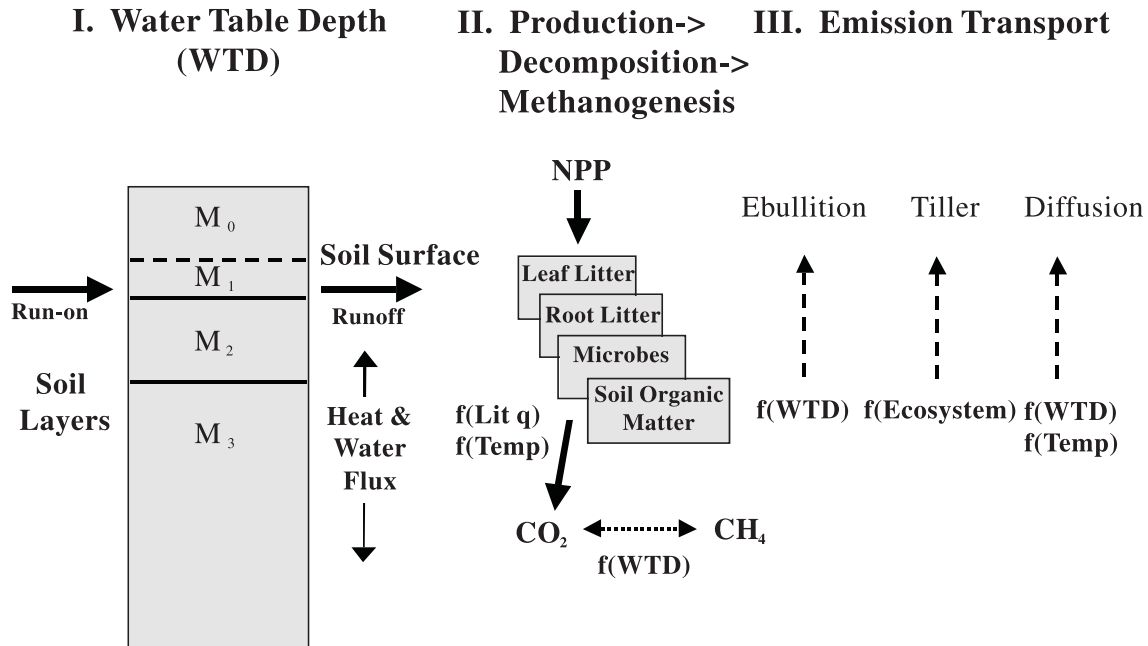
In this paper, we report on results from a daily simulation model that attempts to address most of these ecosystem control components on carbon cycling and trace gas (CH<sub>4</sub> and CO<sub>2</sub>) emissions in applications at two BOREAS study areas, old black spruce (*Picea mariana* (Mill.) BSP) (OBS) forest and fen. These sites are both potentially important sources of methane flux in the boreal ecosystem (Moosavi and Crill 1997). The ecosystems differ significantly, however, in terms of vegetation composition and surface geomorphology. Through comparisons of modeled and measured flux estimates for water, CO<sub>2</sub>, and CH<sub>4</sub>, we can evaluate alternative methods and algorithms for determining boreal biome–atmosphere exchange. The main objectives of this modeling study were to (i) evaluate the performance of the National Aeronautics and Space Administration (NASA) – Carnegie–Ames–Stanford Approach (CASA) simulation model against water and carbon fluxes measured independently at BOREAS field sites, (ii) refine the concepts and algorithms upon which this generalized scheme for soil trace gas emissions can be built, and (iii) evaluate requirements to scale-up model results and extrapolate interannual trace gas flux estimates over the entire North America boreal forest region, relying on satellite data to characterize properties of the land surface.

## Model background description

The daily NASA–CASA model is an aggregated representation of major ecosystem carbon and nitrogen (N) transformations and trace gas fluxes (Potter 1997). It includes interactions of gas flux controls: nutrient substrate availability, soil moisture, temperature, texture, and microbial activity. The model is designed to simulate daily and seasonal patterns in net carbon fixation, nutrient allocation, litter fall, and soil nutrient mineralization, and CO<sub>2</sub> exchange, in addition to CH<sub>4</sub> production, consumption, and emission. A complete description of the previous model design is provided by Potter and Klooster (1997) and Potter (1997).

For application in this study, several model components of the daily NASA–CASA version described by Potter (1997) remain unchanged. For example, the carbon–methane flux module has been designed for seasonally inundated ecosystems with three main subcomponents (Fig. 1): (i) soil temperature and water table depth (WTD) predicted as a function of moisture inputs and field capacity of poorly drained organic soils, (ii) CH<sub>4</sub> production within the anoxic

**Fig. 1.** Schematic representation of components in the methane emission model. The wetland soil profile (I) is layered with depth into a surface ponded layer ( $M_0$ ), a surface organic layer ( $M_1$ ), a surface organic–mineral layer ( $M_2$ ), and a subsurface mineral layer ( $M_3$ ). The production and decomposition component (II) shows separate pools for carbon cycling among pools of leaf litter, root litter, woody detritus, microbes, and soil organic matter. Microbial respiration rate is controlled by temperature ( $T$ ) and litter quality ( $q$ ), whereas coupled production of methane within the anoxic soil layers is a function of water table depth (WTD). Three pathways in the component (III) for gaseous methane emission are molecular diffusion, ebullition, and plant vascular transport.



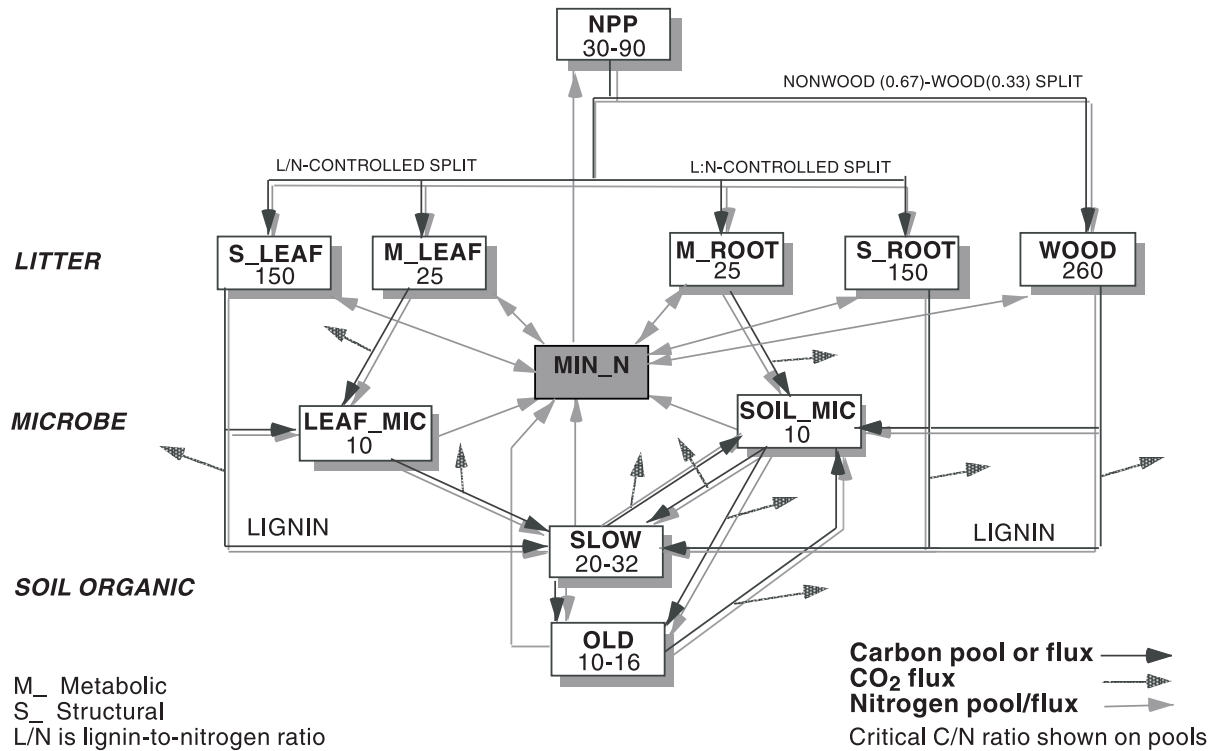
soil layer predicted as a function of WTD and  $\text{CO}_2$  production (from litter decomposition) under poorly drained conditions, and (iii)  $\text{CH}_4$  gaseous transport pathways (molecular diffusion, ebullition, and plant vascular transport) for stored soil methane predicted as a function of WTD, seasonal plant cover, and ecosystem type. The design of the model is expressly for use with remotely sensed inputs of vegetation cover, plant stand production, phenology, litter fall, and surface hydrology over broad spatial extents. Consumption of  $\text{CH}_4$  in relatively well-drained soil profiles is simulated independently in NASA–CASA using a modified version of Fick's first law based on computations for diffusivity in aggregated media (Potter et al. 1996), together with the daily soil water balance model. These algorithms are applicable for estimation of oxidative methane consumption in better drained topographic sites in the BOREAS study areas.

Other key model features from the NASA–CASA version described by Potter (1997) include the monthly fraction of overstory net primary production (NPP), defined as net fixation of  $\text{CO}_2$  by vegetation, is computed on the basis of light-use efficiency (Monteith 1972). New production of plant biomass is estimated as a product of intercepted photosynthetically active radiation (IPAR) and a light utilization efficiency term ( $\epsilon_{\text{max}}$ ) that is modified by temperature and soil moisture. Freeze–thaw dynamics with soil depth operate according to the degree-day method of Jumikis (1966), as described by Bonan (1989). Conversion from mean temperature of air ( $T_a$ ) to temperature at the litter–soil surface ( $T_s$ ) follows empirical relationships reported by Yin and Arp (1993). The computed fraction of water-filled pore space (WFPS; defined as the ratio of volumetric water content to

saturation capacity) in moss, humus, and mineral soil layers is used to calculate scalars that represents the effect of soil moisture on organic matter turnover and  $\text{CO}_2$  emission rates, following the litter decomposition algorithms developed by Doran et al. (1990).

For the soil carbon cycling component (Fig. 2), our design remains comparable with a somewhat simplified version of the CENTURY ecosystem model (Parton et al. 1992), which simulates soil C cycling with a set of compartmental difference equations. First-order equations simulate heterotrophic respiration fluxes of  $\text{CO}_2$  and exchange of decomposing plant residue (metabolic and structural fractions) at the soil surface, together with surface soil organic matter (SOM) fractions that presumably vary in age and chemical composition. Active (microbial biomass and labile substrates), slow (chemically protected), and passive (physically protected) fractions of the SOM are represented. In the CASA model, as with many other ecosystem models, C and N cycling are considered to be tightly coupled, with NPP considered a useful model driver for nutrient transformation rates. The effect of temperature on microbially controlled litter and soil C and N mineralization fluxes was defined as an exponential response using a  $Q_{10}$  (the multiplicative increase in soil biological activity for a  $10^\circ\text{C}$  rise in temperature), with a value of 1.5 for surface litter decomposition and a value of 2.0 for soil decomposition (Raich and Potter 1995; Potter 1997). Following measurements reported by Hogg et al. (1992), a soil temperature level of  $12^\circ\text{C}$  was used to set the near-optimum  $Q_{10}$ -based litter decomposition scalar for peatland organic matter. To estimate total  $\text{CO}_2$  fluxes from soil, including root respiration sources, the algorithm derived by

**Fig. 2.** Litter and soil C and N transformations in the model, which lead to substrates for trace gas production. Structure follows the CENTURY model of Parton et al. (1992). Carbon pools are outlined in black and labeled with C/N ratios, C fluxes are solid arrows, CO<sub>2</sub> production are stippled arrows; nitrogen pools are shaded; and N fluxes are shaded arrows. Levels of litter, microbe (MIC), and soil organic (SLOW and OLD) pools are shown. Structural (S) and metabolic (M) pools are shown for leaf and root litter.



Raich and Potter (1995) was applied for prediction of daily soil respiration.

The NASA-CASA model for BOREAS sites differs in a number of ways from the SPAM model of Frohling et al. (1996), which was developed for CO<sub>2</sub> flux studies of spruce-moss sites in BOREAS. For example, NASA-CASA has dual, instead of a single, exponential decay pools for root litter and humus decomposition, neither of which have been calibrated specifically using boreal site data. Unlike SPAM, NASA-CASA is designed with mechanisms for potential upward movement of the water table and horizontal inflows of surface water depending on microtopography, both of which influence methane flux rates. There are other notable differences in the two models' algorithms for moisture interception and evapotranspiration, soil freeze-thaw dynamics, water retention mechanisms, litter fall timing, and litter quality controls on SOM decomposition rates.

### Refinements for BOREAS ecosystem simulations

To more accurately represent ecosystem controls and soil processes for boreal forest carbon cycles, several modifications are introduced in this study for the NASA-CASA soil hydrology and nutrient cycling model described by Potter (1997). These changes include refinement of ecosystem water balance equations, carbon and water relations of the living ground cover and humus, and soil temperature controls on organic matter decomposition rates.

### Water balance equations

To estimate plant and soil water balance in the previous versions of the model, we used a formulation of the empirical Priestly and Taylor (1972) evapotranspiration equation developed by Campbell (1977) and Bonan (1989). However, plant physiological measurements during BOREAS show that atmospheric desiccation can result from the forest's strong biological control limiting surface evaporation (Hall et al. 1996).

Hence, for this study, a more physiologically based daily potential evapotranspiration (PET) flux for the canopy is estimated using a Penman-Monteith algorithm derived according to the methods described by Woodward (1987) and Monteith and Unsworth (1990):

$$[1] \quad \text{PET} = \frac{[(R_{\text{net}} s) + (\rho c_p (e_s(T_a) - e) / r_a)]}{[s + \gamma(r_a + r_s) / r_a]}$$

where  $R_{\text{net}}$  is the daily net shortwave radiation flux to the canopy ( $\text{W}\cdot\text{m}^{-2}$ ),  $s$  is the rate of change of saturation vapor pressure with temperature ( $\text{mbar}/^\circ\text{C}$ ),  $\rho$  is the density of air ( $\text{kg}\cdot\text{m}^{-3}$ ),  $c_p$  is the specific heat of air ( $\text{J}\cdot\text{g}^{-1}\cdot^\circ\text{C}^{-1}$ ),  $(e_s(T_a) - e)$  is the difference in water vapor pressure (mbar) between ambient air ( $e$ ) and air at saturation ( $e_s(T_a)$ ),  $\gamma$  is the psychrometric constant ( $\text{mbar}/^\circ\text{C}$ ),  $r_a^{-1}$  is the boundary layer resistance ( $\text{s}\cdot\text{m}^{-1}$ ), and  $r_s^{-1}$  is the stomatal resistance to water vapor ( $\text{s}\cdot\text{m}^{-1}$ ) in the canopy. Model settings for maximum conductance in the canopy conform to observed values for boreal ecosystem sites, as reported by Saugier et al. (1997).

Stomatal conductance is computed for up to five canopy layers, depending on leaf area density.

In addition, daily evaporation flux from the ground cover ( $E_{gc}$ ) surface, typically a living bryophyte (moss) layer with near continuous surface coverage, is estimated from a simplified Penman version (Monteith and Unsworth 1990) of eq. 1, driven by radiation flux through the overstory canopy. The main difference between eq. 1 and  $E_{gc}$  is that the term for stomatal conductance to water vapor in the canopy is absent from this  $E_{gc}$  evaporation flux calculation. This is based on the assumption that mosses, as nonvascular plants, lose water principally by evaporation.

Estimated evapotranspiration flux (ET) for the stand is calculated by comparing daily canopy PET plus  $E_{gc}$  to the multilayer model estimate for daily soil moisture content. It is assumed that canopy PET demand can be satisfied after the  $E_{gc}$  daily evaporation flux from ground cover layers is allowed to adequately dry down the surface moisture supply.

The soil profile is treated as a series of three layers:  $M_1$  is the living moss (ground cover) surface,  $M_2$  is humified organic matter under the moss surface layers, and  $M_3$  is the mineral subsoil (Fig. 1). These layers can differ by ecosystem type in terms of bulk density, moisture holding capacity, texture, and C–N storage. Where drainage is impeded, water can accumulate upwardly in a ponded layer ( $M_0$ ) above the living moss surface.

Water balance in each of the organic and mineral soil layers is modeled as the difference between net inputs of precipitation (PPT) and run-on of water from neighboring microtopographic units (plus, in the case of lower soil layers, addition of volumetric percolation inputs), and outputs of ET, followed by drainage for each profile layer. The amount of water run-on to the profile from neighboring microtopographic units of equivalent area is calibrated using a multiplier variable ( $\beta$ ) on the daily PPT and snowmelt inputs, which is adjusted to reproduce BOREAS site measurements for seasonal dynamics of the water table, namely timing and magnitude of maximum daily WTD for the growing season. For fen areas, WTD in both hummock (a mounded rise of organic matter and vegetation) and hollow microtopographic units can be simulated with different settings for the  $\beta$  multiplier variable.

In the absence of a rising WTD, all moisture inputs and outputs are assumed to progress from the surface layer downward. Inputs from rainfall can recharge the organic and mineral soil layers to estimated field capacity (FC). For organic layers, FC is estimated by the product of bulk density and measured water-holding capacity of moss and humus at BOREAS sites (Price et al. 1995). Where drainage is unimpeded, excess water percolates through to lower layers and may eventually leave the system as runoff.

### Snowmelt table depth

Snow dynamics algorithms from the regional hydroecological simulation system (RHESys) developed by Coughlan and Running (1997) have been added to the NASA–CASA model to improve predictions of snow accumulation rate, and the timing and flow rates of spring snowmelt at BOREAS sites. These snow algorithms were developed to improve estimates of annual forest snow hydrology for point and regional calculations of annual forest

productivity. Model algorithms depend upon surface air temperature, solar insolation, precipitation inputs, and canopy leaf area to compute snowpack water equivalent, snow thermal content, albedo, and ablation from snow melt and sublimation fluxes. Snow accumulation rates are dependent on estimated nighttime air temperatures. A heat summation function is used for estimation of snow thermal content to determine when the snowpack is isothermal. The RHESys snow model has been successfully tested at 10 snow telemetry (SNOTEL) stations in the western United States (Coughlan and Running 1997). Comparisons of simulation results to published snow depletion dates have shown that the snow model accurately predicts the relative ranking and magnitude of depletion for different combinations of forest cover, elevation, and aspect.

### Ground cover productivity

The moss ground cover layer growing on the forest floor has been identified as an important component of the boreal carbon cycle (Oechel and van Cleve 1986; Johnson and Damman 1993). In BOREAS black spruce stands, nonvascular plants may account for at least 15–25% of the annual C uptake (Hall et al. 1996), and the percentage may be even higher in fen ecosystems. Therefore, to simulate seasonal patterns in net primary production (NPP) for the moss ground cover layer, we adapted the NASA–CASA model algorithm described by Potter and Klooster (1997) for ground cover production estimates.

Daily  $NPP_{gc}$  is estimated as a product of cloud-corrected surface solar irradiance ( $S$ ), fractional intercepted photosynthetically active radiation (FPAR) by the overstory canopy, and a maximum light use efficiency term ( $\epsilon_{gc}$ ) for moss, modified by temperature ( $T$ ) and moisture ( $W_{gc}$ ) stress scalars, as expressed in the following equation:

$$[2] \quad NPP_{gc} = S(1 - FPAR)\epsilon_{gc}TW_{gc}$$

An estimated maximum  $\epsilon_{gc}$  value of  $0.06 \text{ g C}\cdot\text{MJ}^{-1} \text{ PAR}$  for moss cover at BOREAS sites is derived from measurements of  $\text{CO}_2$  exchange in a black spruce stand (Goulden and Crill 1997). The  $T$  stress term is computed with reference to a derivation of optimal air surface temperatures ( $T_{opt}$ ) for plant growth (Potter et al. 1993). Over the globe,  $T_{opt}$  settings range from near  $0^\circ\text{C}$  in the Arctic to near  $35^\circ\text{C}$  in low-latitude deserts.

Our estimation of the moisture control function for  $W_{gc}$  is derived from water balance in the  $M_1$  organic soil layer following a parabolic physiological response similar to that proposed by Froelking et al. (1996):

$$[3] \quad W_{gc} = [-0.0006(\text{FC} - 50)^2] + 1$$

where the optimal moss water content for primary production, expressed as a percentage of FC, occurs at around 50% by volume water.

Moss litter contributions to decaying organic matter pools was set equal to the annual production estimate for the moss ground cover layer. Lacking better information, partitioning of ground cover litter biomass between decomposing leaf and root pools was set at a constant ratio of 60:40.

**Table 1.** Estimated NASA–CASA parameter settings and sources for BOREAS simulations.

Model parameter	Units	NSA OBS	NSA fen
<b>Geographic</b>			
Latitude and longitude		55.88°N, 98.48°W	55.91°N, 98.42°W
Elevation	m	259	211
<b>Overstory vegetation</b>			
Leaf nitrogen content	percent	0.7 (2, 3)	0.5*
Leaf lignin content	percent	28.2	10.0*
Maximum stomatal conductance	mm·s <sup>-1</sup>	1.0 (2,14)	5.0 (13)
Maximum C fixation efficiency	g C·MJ <sup>-1</sup>	0.25–0.4 (4)	0.4*
One-sided maximum LAI	m <sup>2</sup> ·m <sup>-2</sup>	4.0 (8, 10)	2.0*
Specific leaf area	m <sup>2</sup> ·(g C) <sup>-1</sup>	0.027 (2, 13)	0.025 (13)
Litter C allocation	%leaf:root:stem	15:25:60 (2)	55:35:10*
Rooting depth	m	0.5 (1, 12)	0.5 (1)
Canopy albedo	unitless	0.1 (6)	0.2 (6)
<b>Ground cover</b>			
Cover type		Mixed moss (11)	<i>Sphagnum</i> moss
Nitrogen content	percent	2.2 (11)	2.2 (11)
Ground cover thickness	m	0.3 (1)	0.5*
Bulk density	g·cm <sup>-3</sup>	0.03 (5, 11)	0.03*
Water-holding capacity	g·g <sup>-1</sup> dry	2.0 (5)	
Thickness of humus (including peat)	m	3.0 (1)	2.0* (1)
Humus bulk density	g·cm <sup>-3</sup>	0.1 (5)	0.1*
Water-holding capacity of humus	g·g <sup>-1</sup> dry	3.5 (5)	
<b>Mineral soils</b>			
Bulk density	g·cm <sup>-3</sup>	0.8 (7)	0.1*
Texture	%sand:silt:clay	26:29:45 (7)	45:50:5*
Minimum water content	% bed volume	22 (5)	
Field capacity	% bed volume	36 (5)	
Total porosity	% bed volume	45 (5)	
Soil depth to permafrost	m	0.5 (1, 12)	2.0 (1)
Total organic carbon	g C·m <sup>-2</sup>	12 000 (9)	

**Note:** Blanks are shown for parameters with no readily available values, in which case the default model value for boreal ecosystems was used (Potter 1999). Sources are given in parentheses: (1) Zoltai et al. (1988); (2) Hunt and Running (1992); (3) Trofymow et al. (1995); (4) Goetz and Prince (1996, 1998); (5) Frohling et al. (1996); (6) Betts and Ball (1997); (7) Burke et al. 1997); (8) Chen et al. (1997); (9) Frohling (1997); (10) Gower et al. (1997); (11) Harden et al. (1997); (12) Kimball et al. (1997); (13) Liu et al. (1997); (14) Saugier et al. (1997).

\*Values are estimated based on the compilation of literature sources cited under this parameter category.

## Model input data and initialization for sites

Initialized state and driver variables used in the model were designed to reproduce, as closely as possible, ecosystem conditions during 1994–1996 at two BOREAS different sites, old black spruce (OBS) forest and fen, both located within the Northern Study Area (NSA) near Thompson, Man. At the NSA, soils are predominantly derived from Glacial Lake Agassiz sediments and consist of clays, organics, and some sandy deposits area (Veldhuis 1998; H. Veldhuis, unpublished data). The topography is generally flat with abundant wetland areas, such that drainage of much of the area is poor. Bog and fen ecosystems occur on most of the low-lying terrain where permafrost is absent. Permafrost occurs a few feet below the surface in upland veneer bogs. It also occurs at a greater depth under thickly wooded slopes. Literature sources from BOREAS were surveyed, and the data values reported therein were compared for determination of representative parameter settings for model initial conditions (Table 1).

Overstory vegetation at the NSA OBS site is about 70–90 years old. Leaf area coverage is relatively homogeneous and

the spruce trees reach a height of approximately 10 m. The ground cover is a mix of feather moss (e.g., *Pleurozium schreberi* (Brid.) Mitt.) with lower level areas of sphagnum peat bog (Harden et al. 1997). Observations at BOREAS sites show that the root zone of conifers is thin (generally <50 cm deep) and is contained entirely within the living and decomposing moss–humus layer.

The NSA fen area nearest to where the tower is located is called a “rich” fen (Bubier et al. 1995a) with no permafrost collapse features. Tamarack (*Larix laricina* (Du Roi) K. Koch) and bog birch (*Betula glandulosa* Michx.) are common tree species found in the open graminoid fen along with sedges (e.g., *Carex* spp.). The ground cover is predominantly brown mosses (e.g., *Drepanocladus*, *Scorpidium* spp.), although sphagnum moss (e.g., *Sphagnum fuscum* (Schimp.) Klinggr) dominates the collapsed “poor” fen and intermediate fen sites and on some hummocks in the rich fen. A collapsed fen or palsa is commonly described as a topographic depression covered by vegetation where the ice has melted and the ground has collapsed (Zoltai et al. 1988). For the purposes of this modeling comparison to measurements, we will focus primarily on the poor-to-intermediate fen areas as

ecosystems of median pH and productivity in the wide range of northern peatland types (Bubier et al. 1998).

Daily climate data sets used for model input have been constructed for BOREAS–NSA sites using meteorological measurement records compiled from the Saskatchewan Research Council's automated meteorological station (Shewchuk 1997) at Thompson, Man. Using the reported 15-min average values for 1994 and 1996, we performed a quality assurance check for data anomalies. Missing data were filled in with observations from the previous 1- to 24-h period. Daily input data for the model were generated from precipitation totals over a 24-h period and by averaging net radiation flux measurements over daylight hours. Other meteorological input parameters were averaged over a 24-h period.

Net primary production (NPP) including moss cover and belowground components of the ecosystem was estimated using parameter settings from Table 1 for the NASA–CASA NPP algorithm (Potter and Klooster 1997). Seasonal patterns of litter fall, plus initial states for forest floor litter pools and soil C pools at the sites were also adopted from methods described by Potter (1997). The model was initialized for litter and soil C and N pool sizes using mean monthly climate drivers for a simulation run time of 100 years. No further “tuning” of internal model variables was necessary to initiate the daily simulations for 1994 and 1996. For example, timing of seasonal frost conditions reported to exist in the organic and mineral soils are allowed to develop in a manner consistent with the model's seasonal freeze–thaw algorithms. We assumed that plant-mediated transport (by sedge) of soil gas dominated the methane emission pathways in the poor and intermediate fen ecosystems, which means that following early season plant growth, the model's oxidation, diffusion, and ebullition processes are largely by-passed following production of CH<sub>4</sub> deeper in the soil profile. With falling water table late in the summer, accelerated CH<sub>4</sub> emissions may occur, mainly by ebullition pathways (Potter 1997).

## Modeling results and interpretation

Simulation model results were generated for diagnostic comparison to field observations and flux measurements collected during the 1994 BOREAS field campaign. Several research teams collected data at the NSA OBS and NSA fen sites. We note that, although the available references for team field work are included below, they may not represent a final analysis of the BOREAS measurement data nor the teams' complete scope of work on the BOREAS project.

The BOREAS experimental teams are categorized numerically according to emphasis on trace gas biogeochemistry (TGB) or tower flux (TF) methods. Time-series measurements of soil temperature and CO<sub>2</sub> flux were made by BOREAS TGB-12 (Winston et al. 1997) and by TF-3 and TGB-1 (Goulden and Crill 1997) at the NSA OBS site, and by TGB-3 (Bubier et al. 1998) and TF-10 (Lafleur et al. 1997) at NSA fen sites. Latent heat flux (LE) measurements were also reported for the NSA OBS stand by TF-3 (Goulden et al. 1997). Moisture dynamics in the ground cover and humus, together (in certain cases) with WTD and methane flux measurements, were made by TF-10 (Price et al. 1995) and TGB-1 (Moosavi and Crill 1997) at NSA OBS

sites, and by TGB-3 (Bubier et al. 1995a, 1995b, 1998) at NSA fen sites.

### Soil temperature

Predicted daily temperatures at 20 cm depth (below ground cover surface) in the soil profile were compared to daily average estimates of soil temperatures measured at this same depth by several field teams at the NSA-OBS site (Fig. 3). Model temperatures closely track values measured by TGB-12 (and by TF-3 for areas of sphagnum moss cover) during the summer growing season (June–September). Predicted soil temperatures were generally warmer than observed during the January–February winter period, although model predictions closely reproduced measured values again during the remaining winter months.

We note that relatively cool summer temperatures predicted at 20 cm soil depth by the model do not represent the potential decoupling of thermal and moisture fluxes observed where the forest ground cover is predominantly feather moss. This is in contrast to areas of sphagnum cover, which tend to remain wetter over the summer months (Harden et al. 1997) and hence appear to better match the heat flux calculations produced by our model (Fig. 3). Drier feather moss areas at OBS sites occur in association with closed forest canopies. Sphagnum moss, which covers about the same total area of forest floor as feather moss at the NSA OBS site, is associated more commonly with scattered areas of stunted black spruce (Goulden and Crill 1997).

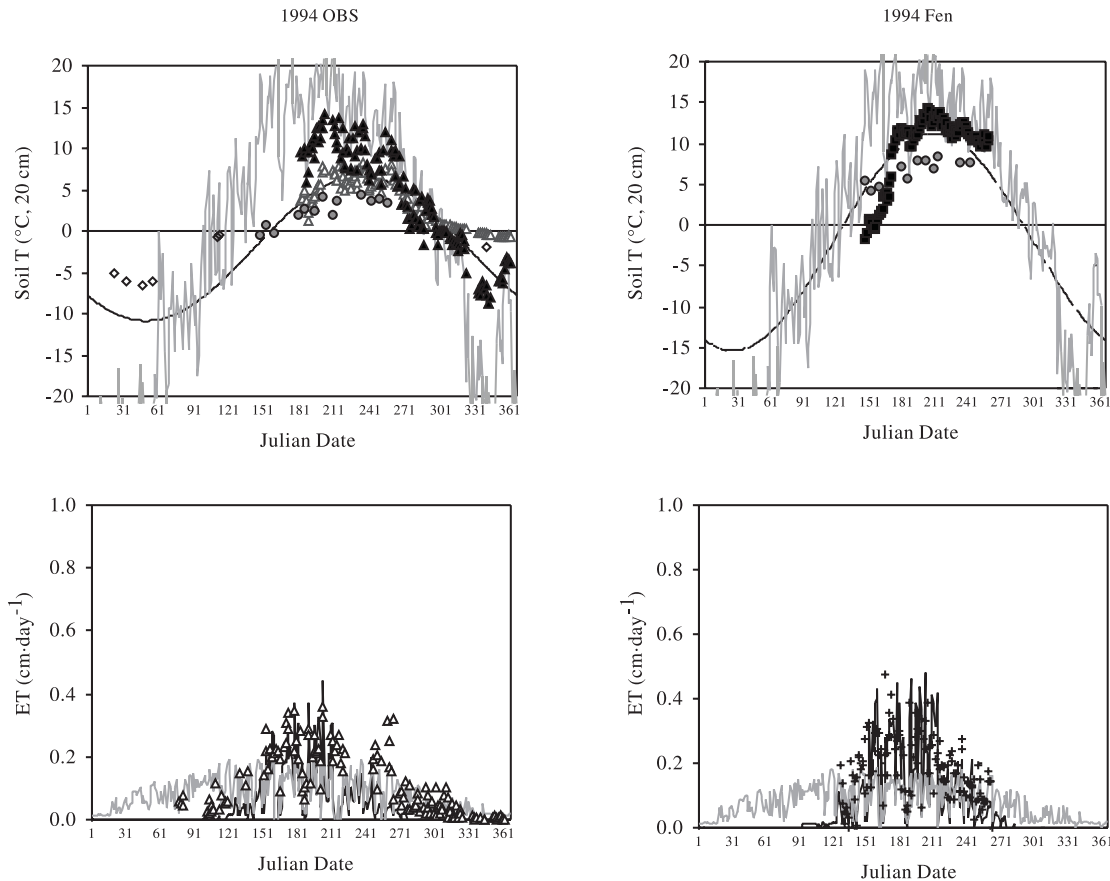
Daily mean soil temperatures at two fen measurement locations are compared in Fig. 3. One location is the small fen area associated with the OBS tower site and measured by TGB-1 in 1994, while the other location is the larger peatland area at the main tower NSA fen site measured by TGB-3. Reported soil temperatures at the NSA fen site are notably higher and more closely track mean surface air temperatures than those at the small OBS fen from about June onward. Model settings required to reproduce the soil temperature patterns measured at the NSA fen site, therefore, must represent soil thermal conditions nearer to the wet ground cover surface than those used for model estimates at the small OBS fen site.

### Snowmelt and water table

In terms of seasonal soil moisture and water table dynamics, timing of snowmelt and the pattern of spring thaw is documented as an important factor controlling early season stand water balance at BOREAS sites. Moss ground cover becomes active as early snowmelt occurs (Bubier et al. 1998), weeks before lower soil layers thaw to tree rooting depth. Depending on microtopographic position, the surface of moss layers may then dry out rapidly as air temperatures warm in the spring. Once the thaw period has ended, summer rainfall appears to penetrate readily through the moss ground cover and mineral sand layers until it reaches an underlying semi-impermeable layer of permafrost, where it subsequently either accumulates upward with a rising water table, or runs off, depending on the local drainage and topography.

For comparisons to our predictions of snowmelt, measurements of changes in snowpack depth at the BOREAS NSA in 1994 indicate that rapid snow loss was underway by

**Fig. 3.** Top panels: Measured mean daily air temperatures (shaded line), predicted soil temperatures at 20 cm depth (black line), and measurements at 20 cm depth by TGB-1 (OBS; shaded circle), TF-3 (OBS; solid triangle, feather moss; open triangle, sphagnum moss), TGB-12 (OBS and OBS fen, open diamond), and TGB-3 (fen; solid square, hollow collapsed fen, collar 2) during 1994. Bottom panels: Predicted ET (solid line, overstory; shaded line, moss ground cover) and ET measurements by TF-3 (OBS; open triangle) and TF-10 (fen; cross). The midnight to midnight average of ET at the OBS site was computed for days during which no fewer than 44 half-hourly flux measurement data points (i.e., >90%) were recorded.



Julian date 100 (mid-April) and continued for about the next 30 days (Levine and Knox 1997). Similarly, our model results predicted snowmelt beginning on Julian date 107 and lasting for the following 31 days. A predicted total of 17.2 cm of water was added to the soil profile over this time period in the snowmelt model run for 1994. The model predicts snowmelt beginning about 14 days later in 1996, the result of colder ( $-1^{\circ}\text{C}$  on average) springtime temperatures compared with 1994.

Results of modeling daily WTD at the NSA OBS site are more difficult to validate than most other diagnostic variables. Moosavi and Crill (1997) reported measurements to suggest that WTD was consistently around  $-25$  cm (negative values are for depths below the ground cover surface) during the 1994 growing season. Our model requires a microtopographic multiplier setting on daily PPT inputs of  $\beta = 0.5$  to closely reproduce this typical pattern of WTD at the OBS site. With this  $\beta$  setting, predicted mean WTD during the 1994 summer growing season was between  $-18$  and  $-36$  cm for the entire year. This implies that water run-on accumulated in the OBS soil profile is derived from neighboring stand areas covering about one half of an equivalent microtopographic unit area in BOREAS spruce stands.

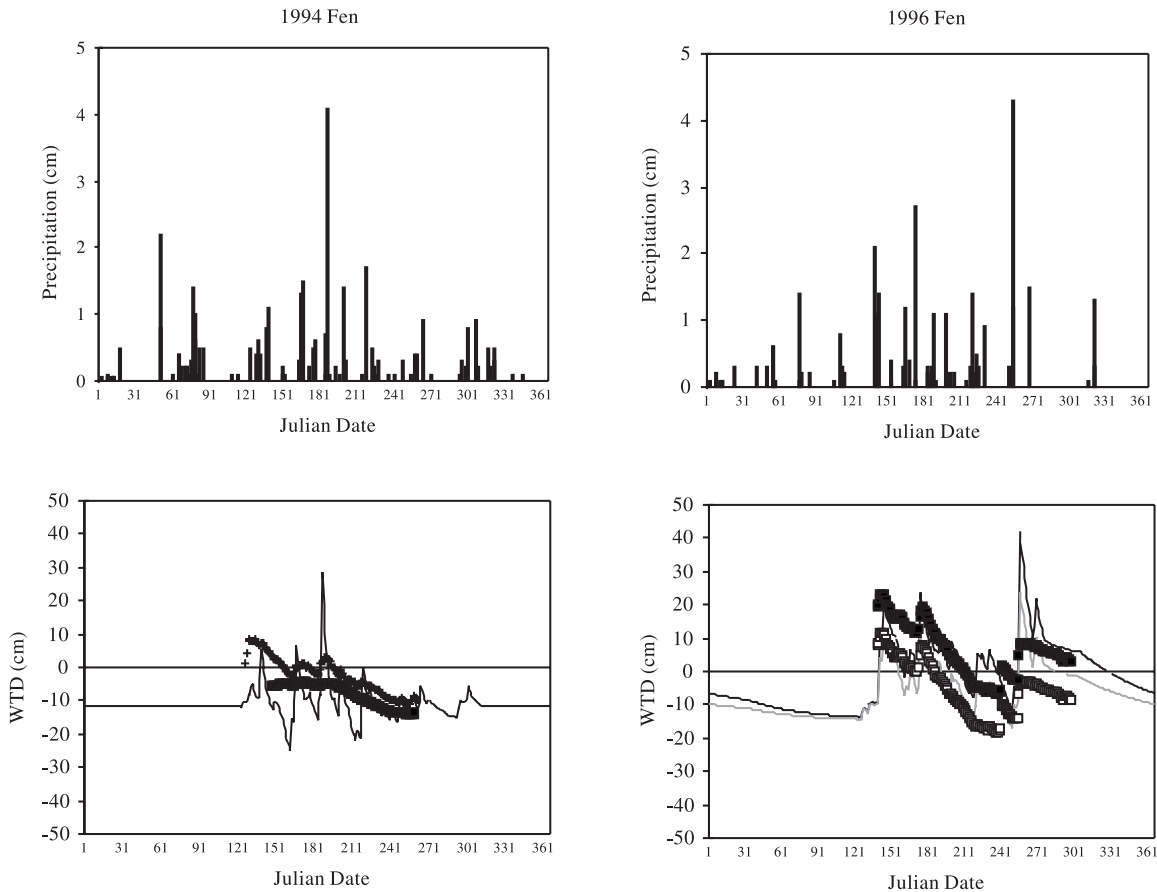
For the NSA fen sites, the soil hydrologic model requires

a microtopographic multiplier setting on daily PPT inputs of  $\beta = 3.2$  or  $4.5$  (depending, respectively, on settings for hummock or hollow location within the fen sites) to most closely reproduce observed patterns of WTD (Fig. 4). Model predictions for WTD compare favorably with peak daily measurements of WTD made in the 1994 growing season (Lafleur et al. 1997) and throughout May–August 1996 (Bubier et al. 1998). Rapid rates of decline in WTD during July and August 1996 can be captured by this simple hydrologic model, but predictions are somewhat less consistent with measured rates of decline in WTD during 1994. In addition, rapid increases in simulated WTD following large precipitation events are not observed in field measurements for early July 1994 nor for mid-September 1996.

### Evapotranspiration

Field measurements during the BOREAS experiment suggest that, although moss and humus layers may remain partially wet for most of the summer growing season, ground cover probably does not exert the major limiting control over transpiration water losses and surface energy balance at the forest stand level during seasonal warming periods. The exception may be in open sphagnum-dominated areas. Instead, relatively low soil temperatures and nutrient-poor soils lead

**Fig. 4.** Top panels: Recorded daily precipitation at Thompson, Man., in 1994 and 1996. Bottom panels: Predicted water table depth (solid line) for NSA fen site and measured depth by TF-10 (cross) and TGB-3 (solid square, hollow collapsed fen, spur 3) in 1994, and by TGB-3 in 1996 (squares) for two microtopographic positions (solid line and solid square, hollow; shaded line and open square, hummock). A measurement of zero represents WTD at the wetland surface, and negative values indicate a WTD below the wetland surface.



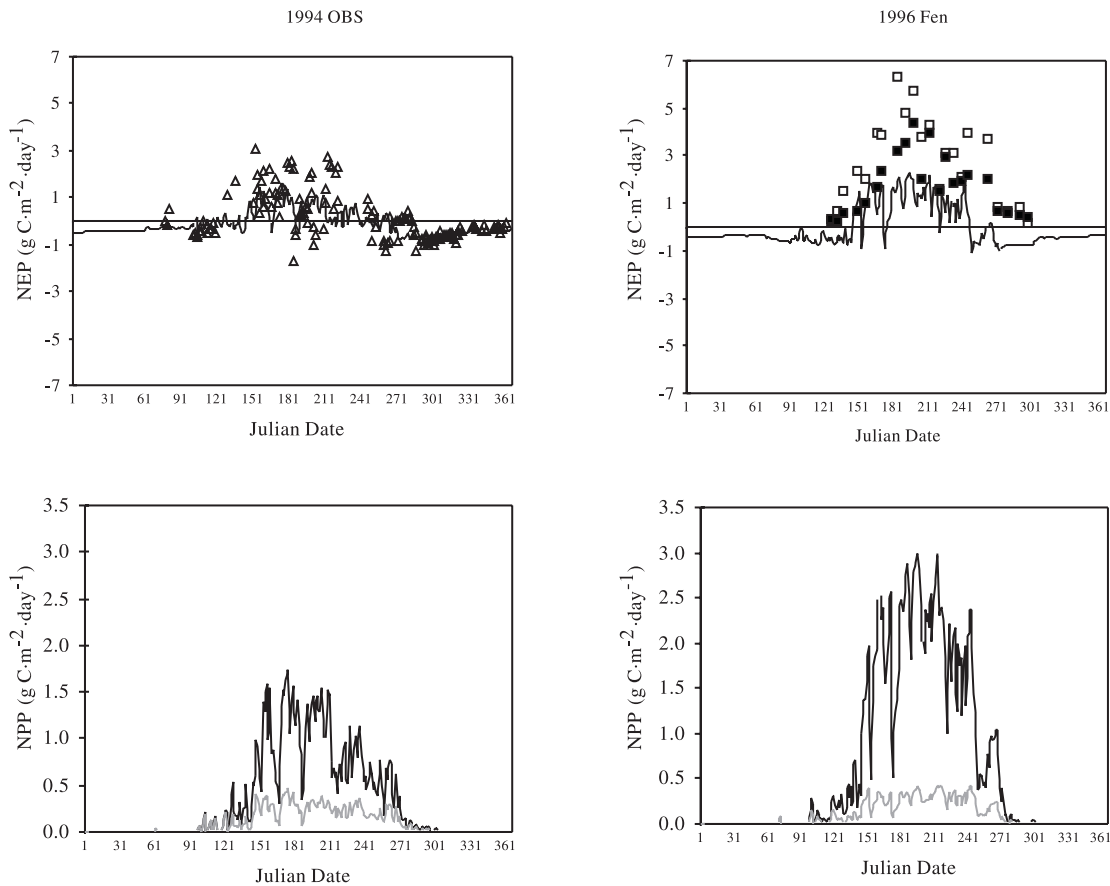
to low seasonal photosynthetic rates in trees, which in turn lead to measurements of slow evapotranspiration rates (i.e., low Bowen ratio) at BOREAS tower sites (Hall et al. 1996). The same trend of low LE flux during midsummer has also been observed at BOREAS fen sites (Lafleur et al. 1997). Much of the available surface energy is dissipated as sensible heat, which often leads to the development of a deep (3000 m) and turbulent summer atmospheric boundary layer. Hence, the boreal forest's strong biological control limiting surface evaporation is a key diagnostic feature for simulation modeling of this ecosystem. The important model variables controlling resistance to LE fluxes should be soil temperature in the spring and atmospheric relative humidity and air temperature in the summer and fall (Hall et al. 1996; Margolis and Ryan 1997).

Our model predictions for daily ET closely track measured flux rates for stand water loss throughout the year at the OBS site (Fig. 3). We estimate the root mean square error (RMSE) for comparison between daily model predictions and measured stand water fluxes to be  $0.015 \text{ cm}\cdot\text{day}^{-1}$ . Predicted ET from spruce trees begins to increase at about the time snowmelt has completed in May and soil temperature (at 20 cm depth) reach positive values ( $^{\circ}\text{C}$ ), a pattern also seen in the measured ET fluxes at the OBS site. Mean daily rates of predicted stand ET are  $0.21 \text{ cm}\cdot\text{day}^{-1}$  during the

growing season months of June through September (compared with a measured mean flux of  $0.19 \text{ cm}\cdot\text{day}^{-1}$ ), with only 6 days reaching what could be considered unrealistically high ET rates of  $>0.5 \text{ cm}\cdot\text{day}^{-1}$  for this stand (Goulden et al. 1997). These 6 days represent the warmest and sunniest conditions observed for the site during the 1994 growing season, with average daily temperatures near or above  $20^{\circ}\text{C}$  and relative humidity readings below 45%. During the cold months of October through May, presumably periods when ET fluxes from trees are minimal, predicted  $\text{ET}_{\text{gc}}$  water losses from the ground cover layer (mean  $0.06 \text{ cm}\cdot\text{day}^{-1}$ ) closely match measured ET rates for the OBS stand. Hence, it appears that the model's ET flux estimates for the stand are strongly controlled by soil temperature during early growing season months and by variability in relative humidity and air temperature during the middle to late growing season.

Rates of ET for fen sites have been reported as higher than forest ET rates at midday (Lafleur et al. 1997). This pattern is also reproduced by the model (Fig. 3) with mean daily rates of predicted stand ET of  $0.27 \text{ cm}\cdot\text{day}^{-1}$  and  $0.39 \text{ cm}\cdot\text{day}^{-1}$  for the NSA fen during the growing season months of 1994 and 1996, respectively. We hypothesize from these model results that, during summer 1996 when potential latent fluxes were higher than in 1994, inundated

**Fig. 5.** Top panels: Predicted net ecosystem production (NEP) of carbon (solid line) and average daily NEP fluxes measured by TF-3 in 1994 (OBS; triangle) and by TGB-3 in 1996 (fen; solid square, hollow; open square, hummock). The midnight to midnight average of NEP at the OBS site was computed for days during which no fewer than 44 half-hourly CO<sub>2</sub> flux measurement data points (i.e., >90%) were recorded. Bottom panels: Predicted net primary production (NPP) for the respective sites and years (solid line, overstory; shaded line, moss ground cover).



fen vegetation would suffer less water stress than spruce stands.

### Net primary production and NEP

Based on previous observations, major limiting factors to primary production at the BOREAS study areas include the relatively short growing season, low light interception by tree canopies (due in part to high foliar clumping), and frozen soils late into the spring warming period. Typical annual NPP for black spruce stands at the NSA has been estimated by Gower et al. (1997) at around 220 g C·m<sup>-2</sup>·year<sup>-1</sup>, and at 152 g C·m<sup>-2</sup> by Frohling (1997) for 1994 simulations. Our model predicts comparable NPP for the NSA OBS site at 158 g C·m<sup>-2</sup>·year<sup>-1</sup> during 1994 and at 135 g C·m<sup>-2</sup>·year<sup>-1</sup> during the 1996, with contributions of 75% from overstory vegetation production and 25% from ground cover production. The springtime months during 1994 were somewhat warmer than those of 1996, which may account for the difference in annual NPP totals between the years. Overall, seasonal model results are consistent with observed production patterns at BOREAS study sites, including the prediction of limited net carbon gain by trees until about the first week of June, followed later by rapid decline of NPP around the end of September, which is indicative of the observed seasonal

asymmetry in NSA OBS ecosystem production (Fig. 5). For fen simulations, we predict annual NPP during 1994 as 250 g C·m<sup>-2</sup>·year<sup>-1</sup> and during 1996 as 270 g C·m<sup>-2</sup>·year<sup>-1</sup>, with about 83% from overstory vegetation production and 17% from ground cover production.

Predicted annual rates of total soil CO<sub>2</sub> flux ( $R_t$ ) and heterotrophic CO<sub>2</sub> flux ( $R_h$ ) are 317 g C·m<sup>-2</sup>·year<sup>-1</sup> and 207 g C·m<sup>-2</sup>·year<sup>-1</sup>, respectively, at the NSA OBS location during 1994 (Fig. 6). Soil  $R_t$  fluxes include both heterotrophic  $R_h$  fluxes and root respiration. Comparison of these soil respiration estimates with measured fluxes is complicated by the high variability in static chamber measurements at locations within the NSA OBS site, which differed in terms of soil temperature (Frohling et al. 1996). Nevertheless, model results generally match the range of measured fluxes for  $R_t$ . Both measured and modeled data sets show less seasonal asymmetry than predicted NPP fluxes and typically higher flux rates (= 0.5 g C·m<sup>-2</sup>·day<sup>-1</sup>) than NPP during nongrowing season months (October–May). Predicted fluxes for  $R_t$  during the coldest months appear to be lower than expected, although there are no measurements of soil respiration fluxes at the NSA OBS site in midwinter for comparative purposes. On an annual basis, we estimate from the modeling results that heterotrophic CO<sub>2</sub> flux ( $R_h$ ) repre-

**Fig. 6.** Top panels: Predicted soil respiration (solid line, heterotrophic; shaded line, total soil); bottom panels: Predicted methane fluxes (solid line, emission 1994; shaded line, consumption 1994; broken line, emission 1996), with daily measured fluxes by TGB-1 (shaded circle) for OBS-left; and OBS fen (right) in 1994, and by TGB-3 (NSA fen (right), solid square 1994 and shaded square 1996). Methane measurements by TGB-3 are an average of up to seven collars in the collapsed fen (CF) located just east of the main trail to the fen tower hut (Bubier et al. 1995a).

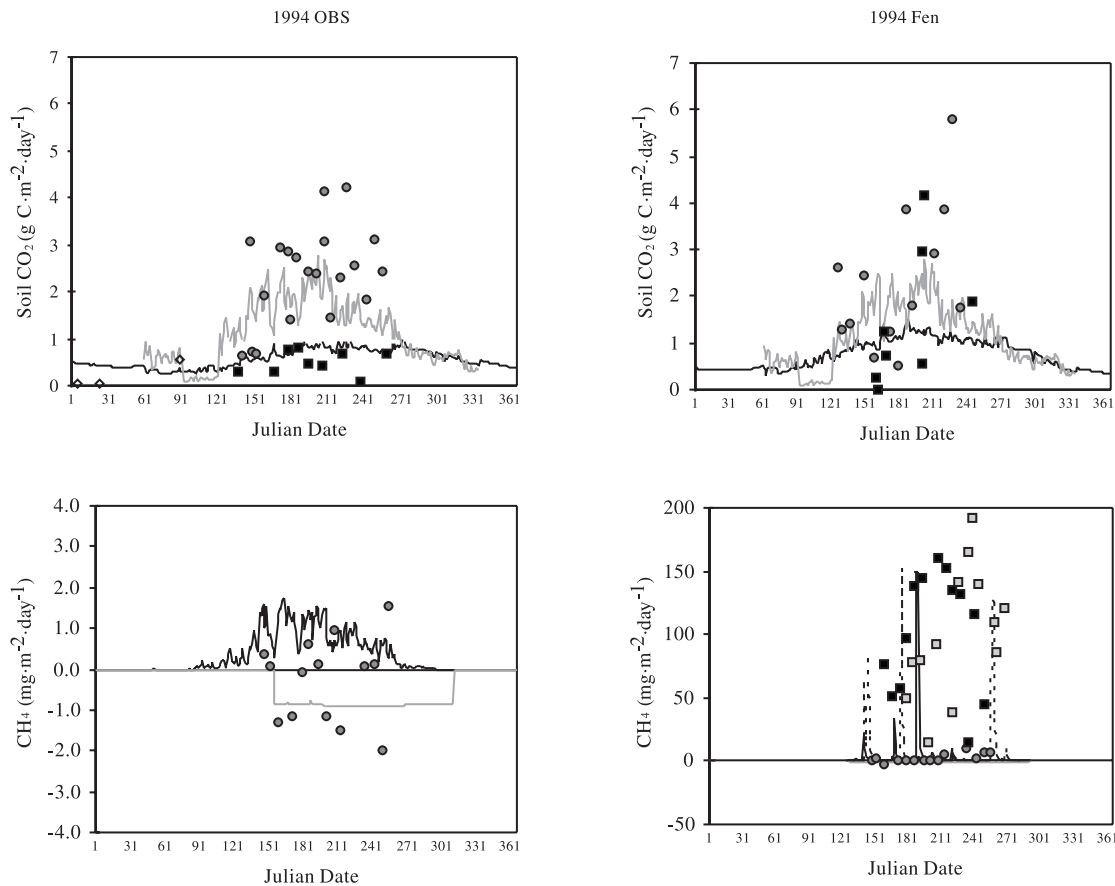


**Table 2.** Mean daily (growing season, June to September) and annual ecosystem fluxes for net carbon dioxide and methane simulated at BOREAS sites.

NSA site	Mean NEP (g C·m <sup>-2</sup> ·day <sup>-1</sup> )		Total NEP (g C·m <sup>-2</sup> ·year <sup>-1</sup> )		Mean methane (mg·m <sup>-2</sup> ·day <sup>-1</sup> )		Total methane (mg·m <sup>-2</sup> ·year <sup>-1</sup> )	
	1994	1996	1994	1996	1994	1996	1994	1996
OBS	0.35	0.30	-49.1	-25.8	-0.79	-0.86	-120	-131
Fen	0.88	0.78	-10.7	-11.8	4.0	5.2	525	827, 329*

\*The first value is for hollows, and the second is for hummocks.

sents about 66% of total soil  $R_t$  fluxes at the NSA OBS during 1994. These same general seasonal patterns in model and measured soil respiration fluxes are found for the NSA fen sites (Fig. 6).

Net ecosystem production (NEP) of carbon is estimated as the difference between NPP and  $R_h$  fluxes. Positive NEP indicates net fluxes of  $\text{CO}_2$  from the atmosphere to the ecosystem, whereas negative NEP indicates net source fluxes of  $\text{CO}_2$  from the ecosystem to the air. Annual integration of daily NEP estimates may be used to characterize the ecosystem in terms of its carbon sink potential. According to previous modeling studies, interannual variability in NEP can be substantial (up to  $\pm 35\%$ ) in the boreal forest (Frolking 1997), a result that is partially the consequence of estimating

a small difference between two relatively large numbers (NPP and  $R_h$ ).

Our seasonal model estimates of NEP are consistent with tower measurements of average daily  $\text{CO}_2$  fluxes at the NSA OBS (Fig. 5). We estimate the RMSE for comparison between daily model predictions and measured  $\text{CO}_2$  exchange flux to be  $1.0 \text{ g C}\cdot\text{m}^{-2}\cdot\text{day}^{-1}$ . Both modeled (Table 2) and measured (Goulden et al. 1997) totals for the year suggest a small net source of ecosystem carbon (NEP between  $-25$  and  $-50 \text{ g C}\cdot\text{m}^{-2}\cdot\text{year}^{-1}$ ) to the atmosphere. Negative NEP estimates from the tower fluxes are reproduced closely by the model for the nongrowing season period. Although predicted growing season fluxes for 1994 track the majority of daily tower estimates for NEP, several high positive esti-

mates are not duplicated by the model. By one way of explanation, we note that it remains to be conclusively determined whether such high tower estimates for daily NEP are an artifact of nighttime measurement biases (low soil respiration estimates) in the tower flux data.

For the NSA fen sites, our model predicts annual NEP of  $-10$  and  $-11$   $\text{g C}\cdot\text{m}^{-2}\cdot\text{year}^{-1}$  for 1994 and 1996, respectively. Seasonal comparisons of measured and modeled fen NEP are presented for 1996 (Fig. 5), in which it appears that the model predictions can closely track net carbon exchange rates for fen hollow sites as estimated by Bubier et al. (1998). As was the case in the NSA OBS comparisons, several high positive NEP measurement estimates are not duplicated by the model. This explains the lower annual NEP predictions for NSA fen areas from the model used here, compared for example to recent carbon sink estimates by Trumbore et al. (1999) of  $31$ – $180$   $\text{g C}\cdot\text{m}^{-2}\cdot\text{year}^{-1}$  NEP in poor and intermediate fens at the BOREAS NSA.

### Methane emission rates

The principal controller that favors high methane emissions observed from BOREAS wetland sites is elevated water table ( $+10$  cm), accompanied by relatively warm soil temperatures and adequate carbon substrate for methanogenesis (Moosavi and Crill 1997). Microtopographic location, defined as hummock versus hollow position within a boreal fen, can strongly influence these environmental controllers (Bubier et al. 1995b).

Peaks in methane emissions predicted by the model coincide with dates of high rainfall input and snowmelt, which raise run-on and elevate WTD to levels of  $+5$  cm and above (Fig. 6). In addition, seasonal patterns of soil  $\text{CH}_4$  emission and uptake fluxes are influenced notably by accumulated soil heat content at both the OBS and Fen sites. For the OBS site, average WTD of below  $-15$  cm throughout the predicted growing season leads to estimation of continuous uptake of  $\text{CH}_4$  by methanotrophic microbes, assumed to be active in the surface soil layers during warm months, at  $\text{CH}_4$  uptake levels consistent with measured rates (Moosavi and Crill 1997). The apparent seasonal timing of  $\text{CH}_4$  uptake is also predicted accurately by the model.

As noted for the previous soil temperature comparisons, two BOREAS fen measurement locations for methane flux are compared in Fig. 6; one is the small fen associated with the OBS tower site measured by TGB-1 in 1994, and the other is at the main tower NSA fen site measured by TGB-3 in both 1994 and 1996. These two fen areas are clearly different in their capacity to act as net methane sources. The smaller, colder fen associated with the OBS stand is probably less productive than the fen tower sites and, therefore, cycles less carbon in the soil during the growing season.

Model predictions for daily and annual  $\text{CH}_4$  flux (Table 2) generally match measured flux levels for both 1994 and 1996. One exception is that the model does not predict elevated methane fluxes into late August 1994, as measured by Bubier et al. (1995a), when both predicted and recorded WTD had declined to near or below the peat moss surface at the NSA fen site. It has been observed in previous field studies that higher  $\text{CH}_4$  fluxes in peatlands can accompany a falling water table (Windsor et al. 1992), and although the

model used here includes this general emission mechanism, apparent high methane outgassing during the late growing season is a characteristic of these boreal fen sites during periods when WTD is falling well below ( $>5$  cm) the peat surface. Modification of the model algorithm for  $\text{CH}_4$  production rates at low WTD can be implemented to represent this  $\text{CH}_4$  emission feature of the BOREAS fen site. Another explanation for high measured  $\text{CH}_4$  emissions late in the growing season could be increased turnover of root biomass in the fen vegetation, creating a pulse of labile carbon for methanogenesis. Once again, alternation in the model algorithms for can be implemented to represent this process of rapid root turnover.

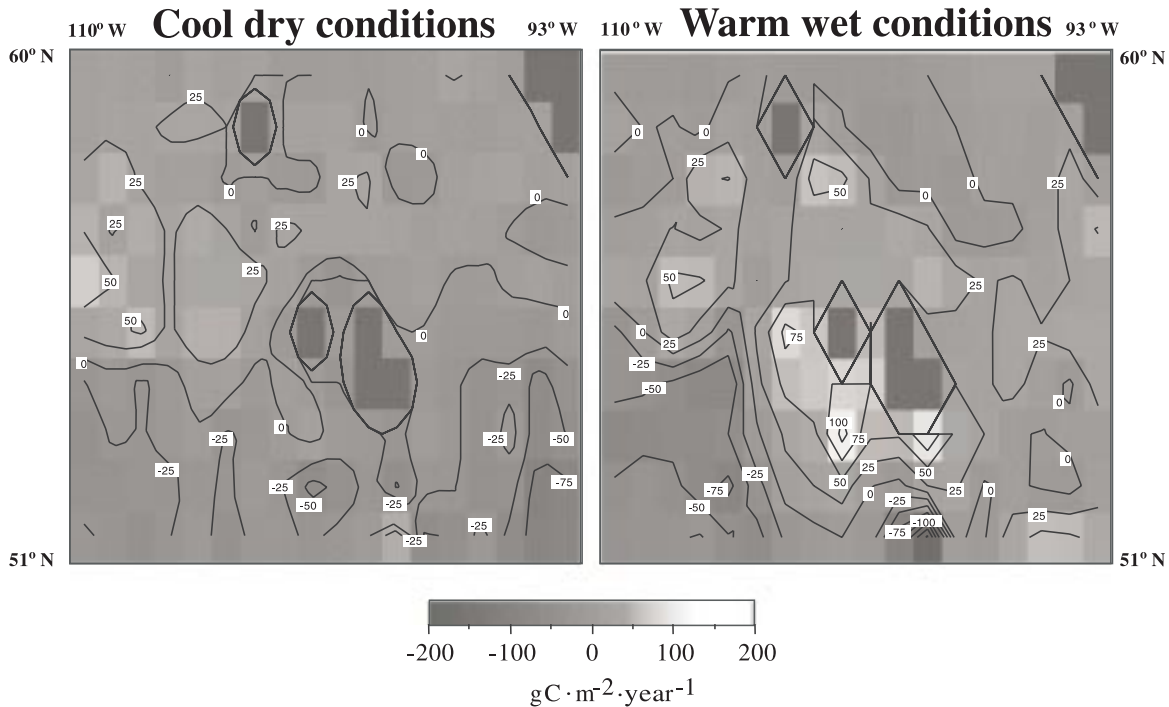
Nevertheless, as consistent with field measurements, predicted  $\text{CH}_4$  fluxes suggest that on average the OBS site was a net sink of  $-0.8$   $\text{mg CH}_4\cdot\text{m}^{-2}\cdot\text{day}^{-1}$  during growing season months, whereas the fen site generated net emissions of  $3$ – $150$   $\text{mg CH}_4\cdot\text{m}^{-2}\cdot\text{day}^{-1}$ . For the OBS site, the model predicts mean daily rates of  $\text{CH}_4$  emission and uptake, respectively, at  $0.20$  and  $-0.85$   $\text{mg CH}_4\cdot\text{m}^{-2}\cdot\text{day}^{-1}$  over the 1994 growing season. This results in an annual predicted net sink of about  $-120$   $\text{mg CH}_4\cdot\text{m}^{-2}\cdot\text{year}^{-1}$  for the spruce stand. The NSA fen site is a predicted annual source of between  $300$  and  $850$   $\text{mg CH}_4\cdot\text{m}^{-2}\cdot\text{year}^{-1}$ , depending mainly on seasonal precipitation patterns, WTD, and microtopographic position. This annual emission flux is consistent with some previous estimates of annual fen  $\text{CH}_4$  emission rates in the boreal region (Roulet et al. 1992b; Vitt et al. 1990) but is lower than others (Moore and Knowles 1990). Fen hollow areas are predicted to emit almost three times more methane during a given year than hummock areas, a pattern that matches closely to the measured difference in mean  $\text{CH}_4$  flux rates reported by (Bubier et al. 1995a, 1995b) for hollow and hummock areas within their NSA tower fen site.

### Sensitivity tests

Model predictions of relatively small annual NEP fluxes, as measured for selected boreal ecosystems (Goulden et al. 1997; Trumbore et al. 1999), are subject to switching from negative (net ecosystem source) to positive (net ecosystem sink) if either of the predicted components of NEP, namely NPP or soil respiration fluxes, can be altered even slightly in responsive to changes in internal model settings. Because boreal forests occupy about 11% of the terrestrial surface, even small errors in estimation of annual NEP at the forest stand level can add up to large extrapolated fluxes for atmospheric carbon at the global level. Therefore, an important use of carbon cycle models is to investigate which ecosystem parameters can potentially cause large swings in annual NEP estimates, for instance from a  $\text{CO}_2$  source to a  $\text{CO}_2$  sink.

We therefore carried out selected sensitivity tests of our model for the OBS site using 1994 daily climate drivers to evaluate the influence of several model settings on predictions of annual NEP. These settings include (i) allocation constants for NPP carbon to wood biomass and woody detritus inputs to decomposing litter carbon pools, which if decreased could lead to lower carbon sink potential for the forest stand; (ii) accumulation rates of total NPP carbon in decaying moss ground cover layers; (iii) precipitation run-on

**Fig. 7.** BOREAS regional model results for NEP in two different climate years. Spatial resolution is  $1^\circ$ , using regional data drivers described in Potter (1999) and Potter and Klooster (1998). Contour lines are labeled in units of  $\text{g C}\cdot\text{m}^{-2}\cdot\text{year}^{-1}$ .



rates for surface water accumulation in the forest soil profile, which would cause a change in WTD in the spruce stand and potentially alter moisture controls on soil organic matter decomposition rates; and (iv) higher stand light utilization efficiency for conversion of surface irradiance to plant fixed carbon, either by altering the empirical  $\epsilon_{\max}$  term in the model NPP equation or by changing the assumed FPAR setting for the forest canopy.

We found that, by decreasing fractional allocation rates of annual NPP carbon to wood biomass pools from the default model setting of 60% to a revised value of 40%, which is consistent with the NSA OBS estimate of woody detritus allocation fraction reported by Gower et al. (1997), a minor change in annual predicted NEP values was observed, with a small increase in the net source of ecosystem carbon from  $-49$  to  $-52 \text{ g C}\cdot\text{m}^{-2}\cdot\text{year}^{-1}$  to the atmosphere. This suggests that for short-term simulations of the forest carbon cycle on the order of a few years, improved estimates of allocation coefficients for NPP carbon to woody detritus pools will not greatly affect the prediction of stand carbon balance. Effects of wood accumulation rates on longer time scales could be different though.

Predicted changes in annual forest NEP were more sensitive to alterations in the accumulation rates of total ground cover NPP in decaying moss ground cover layers. To be consistent with the full range of results from Trumbore and Harden (1997), we set detrital accumulation rates to 45% for estimated annual C inputs of moss production, compared with the default model setting 30%. Under these conditions, the net source flux of ecosystem carbon decreased by about 30% to  $-34 \text{ g C}\cdot\text{m}^{-2}\cdot\text{year}^{-1}$  NEP. These findings indicate the relative sensitivity of the model NEP results to the procedure used to initialize the below ground and surface pools of carbon. The potential influence of stand age characteristics and

initialization on model results is investigated in more detail by Potter et al. (2001).

We observed a more modest effect on the predicted net source flux of ecosystem carbon from a change in the surface water accumulation in the forest soil profile. By reducing the microtopographic multiplier setting on daily PPT inputs to a value of  $\beta = 0$ , annual NEP was changed slightly to  $-51 \text{ g C}\cdot\text{m}^{-2}\cdot\text{year}^{-1}$ , which suggests that the marginally drier soil conditions weakly increase carbon turnover rates in the litter and soil organic matter pools.

By far the largest effect on predicted NEP was generated by changing the model settings for light utilization efficiency in the forest canopy. With a change in either the value of our model  $\epsilon_{\max}$  term to 0.4 or canopy FPAR to 0.9, values consistent with high end of measured ranges reported in BOREAS spruce stands by Cihlar et al. (1997) and Goetz and Prince (1998), annual NEP was changed from a net source of C to the atmosphere to a net ecosystem sink of about  $22 \text{ g C}\cdot\text{m}^{-2}\cdot\text{year}^{-1}$ . Hence, this sensitivity analysis suggests that those stand characteristics most closely coupled with NPP inputs to the ecosystem carbon cycle will most strongly affect the prediction of net  $\text{CO}_2$  exchange over the short periods of several years.

## Regional application results

The evaluation of simulation results at the site level is a necessary precursor to extrapolation of flux predictions across larger areas. Subsequent approaches to scaling-up model results for trace gas flux estimates over the entire North America boreal forest region will rely heavily on integration of satellite data to characterize properties of the land surface, such as FPAR. We have previously quantified potential errors in spatial data layers used as regional model in-

puts for BOREAS (Potter et al. 1999), as independent from prediction errors that may result from model design or process algorithms (this study). Our analysis of land cover, hydrology, and soils maps generated as part of the BOREAS project suggests that coverages for plant functional types, derived from a combination of Landsat Thematic Mapper (TM) and Advanced Very High Resolution Radiometer (AVHRR) satellite images, provide the highest quality information to define ecosystem model parameters over the region.

As first model application over the entire BOREAS region, we have upscaled NASA-CASA predictions of NEP for several years using the monthly AVHRR vegetation index to estimate changes in FPAR at a 1° spatial resolution. Regional data drivers used here are essentially the same as those described in Potter (1999) and Potter and Klooster (1998). In summary, complete AVHRR data sets for the 1980s have been produced from National Oceanic and Atmospheric Administration (NOAA) Global Area Coverage (GAC) level 1B data. For surface temperature and precipitation drivers, long-term (1931–1960) average values from Leemans and Cramer (1990) were adjusted using monthly 1° climate anomalies for the period 1980–1988 (Dai and Fung 1993). Average monthly solar irradiance data was obtained from Bishop and Rossow (1991) for the BOREAS region.

Comparison of two different climate years (Fig. 7) suggest that, under wetter precipitation conditions, the model predicts regional NEP to become more positive, as the result of strong relative decreases in soil respiration associated with higher moisture inputs, compared with small changes in predicted NPP fluxes. Under warmer temperature conditions, predicted regional NEP can become a stronger net C source, resulting from higher predicted  $R_h$  fluxes and small declines in NPP. Under conditions of increased surface irradiance associated with warmer temperatures, increases in predicted NPP during the spring (March, April, May) period can generate a higher net annual NEP sink over the BOREAS region.

In our next phase of regional modeling, higher resolution (30-m) remote sensing information will be critical for boreal ecosystem simulations of small “patch” types (e.g., dry conifer, fen, and disturbed sites) that are frequently obscured at the 1-km pixel resolution of AVHRR. For improving our regional upscaling approach, it will be necessary to include simulation results for these small patches by extrapolating predicted fluxes in proportion to their area coverage percentages (Landsat TM source) throughout the boreal region.

## Conclusions

Validation of model predictions for water and temperature variables at BOREAS sites suggest that overall correlations between daily predictions and measurements are high, with  $r^2$  values of 0.54 and 0.78 for regressions of ET fluxes ( $n = 68$ ) and soil temperature ( $n = 76$ ) during 1994, respectively. Nevertheless, there is substantial variability between independent field measurements of the same environmental variable within the same BOREAS sites, which restricts more definitive validation of model predictions for WTD, soil respiration, and NEP fluxes. Differences between predicted and measured daily fluxes of  $\text{CO}_2$  and methane were occasion-

ally on the order of 50%, which may be attributable to limited model information on within-site microtopographic characteristics of the measured vegetation, ground cover, and soils.

The NASA-CASA model is designed to use remotely sensed ecosystem type and vegetation properties (FPAR and leaf area index) directly, together with gridded climate inputs, to drive simulations of soil trace gases and NEP over several years (Potter and Klooster 1998) and under future climate change scenarios. It is clear from the site-level evaluation of the model presented in this paper that certain internal variables should be carefully assigned to boreal ecosystem types as the simulations are scaled-up to a regional level. Specifically, ecosystem settings for average microtopographic effect of water run-on and runoff can affect estimates of WTD and net methane emissions. Within fen sites, hollow and hummock areas should be treated differently in terms of this microtopographic effect. Likewise, results of ET simulations suggest that the ecosystem setting for maximum stomatal conductance makes a difference in correctly regulating overall stand water balance. Further information being developed by BOREAS investigators on the properties of moss and lichen ground covers will be useful additions to the spatial data base to support regional simulations of the boreal water and carbon cycles.

## Acknowledgments

This work was supported by grants from the NASA Terrestrial Ecology Program (BOREAS Guest Investigator) and from the NASA Land Surface Hydrology Program. Thanks to Joseph Coughlan for guidance in the implementation of snowmelt algorithms. Steve Froelking provided valuable assistance in the presentation of field flux measurements. The data and assistance provided by all members of BOREAS field teams HYD-8 (L.E. Band et al.), TF-3 (S.C. Wofsy et al.), TF-10 (P.M. Lafleur et al.), TGB-1 (P.M. Crill et al.), TGB-3 (T.R. Moore et al.), and TGB-12 (J.W. Harden et al.) is gratefully acknowledged.

## References

- Bachand, R., Moore, T.R., and Roulet, N.T. 1996. A map of methane emissions from wetlands in Canada. Centre for Climate and Global Change Research, McGill University, Montréal, Que. Rep. 96-7.
- Bartlett, K.B., and Harriss, R.C. 1993. Review and assessment of methane emissions from wetlands. *Chemosphere*, **26**: 261–320.
- Betts, A.K., and Ball, J.H. 1997. Albedo over the boreal forest. *J. Geophys. Res.* **102**(D24): 28 901 – 28 909.
- Bishop, J.K.B., and Rossow, W.B. 1991. Spatial and temporal variability of global surface solar irradiance. *J. Geophys. Res.* **96**: 16 839 – 16 858.
- Bonan, G.B. 1989. A computer model of the solar radiation, soil moisture and soil thermal regimes in boreal forests. *Ecol. Modell.* **45**: 275–306.
- Bonan, G.B. 1991. Atmosphere-biosphere exchange of carbon dioxide in boreal forest. *J. Geophys. Res.* **96**: 7301–7312.
- BOREAS Science Team. 1995. BOREAS science white papers. NASA, Washington, D.C.
- Bubier, J.L., Moore, T.R., Bellisario, L., Comer, N.T., and Crill, P.M. 1995a. Ecological controls on methane emissions from a northern peatland complex in the zone of discontinuous perma-

- frost, Manitoba, Canada. *Global Biogeochem. Cycles*, **9**: 455–470.
- Bubier, J.T., Moore, R., and Juggins, S. 1995*b*. Predicting methane emissions from bryophyte distribution in northern Canadian peatlands. *Ecology*, **76**: 677–693.
- Bubier, J.L., Crill, P.M., Moore, T.R., Savage, K., and Varner, R.K. 1998. Seasonal patterns and controls on net ecosystem CO<sub>2</sub> exchange in a boreal peatland complex. *Global Biogeochem. Cycles*, **12**: 703–714.
- Burke, R.A., Zepp, R.G., Tarr, M.A., Miller, W.L., and Stocks, B.J. 1997. Effect of fire on soil–atmosphere exchange of methane and carbon dioxide in Canadian boreal forest site. *J. Geophys. Res.* **102**(D24): 29 289 – 29 300.
- Campbell, G.S. 1977. *An introduction to environmental biophysics*. Springer, New York.
- Chen, J.M., Rich, P.M., Gower, S.T., Norman, J.M., and Plummer, S. 1997. Leaf area index of boreal forests: theory, techniques and measurements. *J. Geophys. Res.* **102**(D24): 29 429 – 29 444.
- Cicerone, R., and Oremland, R. 1988. Biogeochemical aspects of atmospheric methane. *Global Biogeochem. Cycles*, **2**: 299–327.
- Cihlar, J., Chen, J., and Li, Z. 1997. Seasonal AVHRR multi-channel data sets and products for scaling up biospheric processes. *J. Geophys. Res.* **102**(D24): 29 625 – 29 640.
- Coughlan, J.C., and Running, S.W. 1997. Regional ecosystem simulation: a general model for simulating snow accumulation and melt in mountainous terrain. *Landsc. Ecol.* **12**: 119–136.
- Dai, A., and Fung, I.Y. 1993. Can climate variability contribute to the missing CO<sub>2</sub> sink? *Global Biogeochem. Cycles*, **7**: 599–609.
- Doran, J.W., Mielke, L.N., and Power, J.F. 1990. Microbial activity as regulated by soil water filled pore space. *In* Transactions of the 14th International Congress of Soil Science, Kyoto, Japan. International Soil Science Society, Kyoto. pp. 94–99.
- Frolking, S. 1997. Sensitivity of spruce/moss boreal forest carbon balance to seasonal anomalies in weather. *J. Geophys. Res.* **102**(D24): 29 053 – 29 064.
- Frolking, S., Goulden, M.L., Wofsy, S.C., Fan, S.-M., Sutton, D.J., Munger, J.W., Bazzaz, A.M., Daube, B.C., Crill, P.M., Aber, J.D., Band, L.E., Wang, X., Savage, K., Moore, T., and Harriss, R.C. 1996. Temporal variability in the carbon balance of a spruce/moss boreal forest. *Global Change Biol.* **2**: 343–366.
- Fung, I., John, J., Lerner, J., Matthews, E., Prather, M., Steele, L.P., and Fraser, P.J. 1991. Three-dimensional model synthesis of the global methane cycle. *J. Geophys. Res.* **96**: 13 033 – 13 065.
- Goetz, S.J., and Prince, S.D. 1996. Remote sensing of net primary production in boreal forest stands. *Agric. For. Meteorol.* **78**: 149–179.
- Goetz, S.J., and Prince, S.D. 1998. Variability in light utilization and net primary production in boreal forest stands, *Can. J. For. Res.* **28**: 375–389.
- Goulden, M.L., and Crill, P.M. 1997. Automated measurements of CO<sub>2</sub> exchange at the moss surface of a black spruce forest. *Tree Physiol.* **17**: 537–542.
- Goulden, M.L., Daube, B.C., Fan, S.-M., Sutton, D.J., Bazzaz, A., Munger, J.W., and Wofsy, S.C. 1997. Physiological responses of a black spruce forest to weather. *J. Geophys. Res.* **102**(D24): 28 987 – 28 996.
- Goulden, M.L., Wofsy, S.C., Harden, J.W., Trumbore, S.E., Crill, P.M., Gower, S.T., Fries, T., Daube, B.C., Fan, S.-M., Sutton, D.J., Bazzaz, A., and Munger, J.W. 1998. Sensitivity of boreal forest carbon balance to soil thaw. *Science* (Washington, D.C.), **279**: 214–217.
- Gower, S.T., Vogel, J., Stow, T., Norman, J., Steele, S., and Kucharik, C. 1997. Carbon distribution and above ground net primary production in aspen, jack pine and black spruce stands in Saskatchewan and Manitoba, Canada. *J. Geophys. Res.* **102**(D24): 29 029 – 29 042.
- Hall, F.G., Sellers, P.J., and Williams, D.L. 1996. Initial results from the Boreal Ecosystem–Atmosphere Study: BOREAS. *Silva Fenn.* **30**: 109–121.
- Harden, J.W., O’Neill, K.P., Trumbore, S.E., Veldhuis, H., and Stocks, B.J. 1997. Moss and soil contributions to the annual net carbon flux of a maturing boreal forest. *J. Geophys. Res.* **102**(D24): 28 805 – 28 816.
- Hogg, E.H., Lieffers, V.J., and Wein, R.W. 1992. Potential carbon losses from peat profiles: effects of temperature, drought cycles, and fire. *Ecol. Appl.* **2**: 298–306.
- Houghton, J.T., Callander, B.A., and Varney, S.K. (Editors). 1992. *Climate change 1992: the supplementary report to the IPCC scientific assessment*. Report of the Intergovernmental Panel on Climate Change. Cambridge University Press, Cambridge, U.K.
- Hunt, E.R., and Running, S.W. 1992. Simulated dry matter yields for aspen and spruce stands in the North American boreal forest. *Can. J. Remote Sens.* **18**: 126–133.
- Johnson, L.C., and Damman, A.W.H. 1993. Decay and its regulation in *Sphagnum* peatlands. *Adv. Bryol.* **5**: 249–296.
- Jumikis, A.R. 1966. *Thermal soil mechanics*. Rutgers University Press, New Brunswick, N.J.
- Kimball, J.S., White, M.A., and Running, S.W. 1997. BIOME-BGC simulations of stand hydrologic processes for BOREAS. *J. Geophys. Res.* **102**(D24): 29 043 – 29 052.
- Lafleur, P.M., McCaughey, J.H., Joiner, D.W., Bartlett, P.A., and Jelinski, D.E. 1997. Seasonal trends in energy, water, and carbon dioxide fluxes at a northern boreal fen. *J. Geophys. Res.* **102**(D24): 29 009 – 29 020.
- Leemans, R., and Cramer, W.P. 1990. The IIASA database for mean monthly values of temperature, precipitation and cloudiness of a global terrestrial grid. International Institute for Applied Systems Analysis, Laxenberg, Austria. IIASA Laxenburg Working Pap. WP-41.
- Levine, E.R., and Knox, R.G. 1997. Modeling soil temperature and snow dynamics in northern forests, *J. Geophys. Res.* **102**(D24): 29 407 – 29 416.
- Liu, J., Chen, J.M., Cihlar, J., and Park, W.M. 1997. A process-based boreal ecosystem productivity simulator using remote sensing inputs. *Remote Sens. Environ.* **62**: 158–175.
- Margolis, H.A., and Ryan, M.G. 1997. A physiological basis for biosphere–atmosphere interactions in the boreal forest: an overview. *Tree Physiol.* **17**: 491–500.
- Monteith, J.L., 1972. Solar radiation and productivity in tropical ecosystems. *J. Appl. Ecol.* **9**: 747–766.
- Monteith, J.L., and Unsworth, M.H. 1990. *Principles of environmental physics*. 2nd ed. Edward Arnold, London.
- Moore, T.R., and Knowles, R. 1990. Methane emissions from fen, bog, and swamp peatlands in Quebec. *Biogeochemistry*, **11**: 45–61.
- Moosavi, S.C., and Crill, P.M. 1997. Controls on CH<sub>4</sub> and CO<sub>2</sub> emissions along two moisture gradients in the Canadian boreal zone. *J. Geophys. Res.* **102**(D24): 29 261 – 29 278.
- Oechel, W.C., and van Cleve, K. 1986. The role of bryophytes in nutrient cycling in the taiga. *In* Forest ecosystems in the Alaska taiga. Edited by K. van Cleve, F.S. Chapin III, P.W. Flanagan, L.A. Viereck, and C.T. Dyrness. Springer-Verlag, New York.
- Parton, W.J., McKeown, B., Kirchner, V., and Ojima, D. 1992. CENTURY user’s manual. Natural Resource Ecology Laboratory, Colorado State University, Fort Collins.
- Potter, C.S. 1997. An ecosystem simulation model for methane

- production and emission from wetlands. *Global Biogeochem. Cycles*, **11**: 495–506.
- Potter, C.S. 1999. Terrestrial biomass and the effects of deforestation on the global carbon cycle. *BioScience*, **49**: 769–778.
- Potter, C.S., and Klooster, S.A. 1997. Global model estimates of carbon and nitrogen storage in litter and soil pools: response to change in vegetation quality and biomass allocation. *Tellus*, **49B**: 1–17.
- Potter, C.S., and Klooster, S.A. 1998. Interannual variability in soil trace gas (CO<sub>2</sub>, N<sub>2</sub>O, NO) fluxes and analysis of controllers on regional to global scales. *Global Biogeochem. Cycles*, **12**: 621–637.
- Potter, C.S., Randerson, J.T., Field, C.B., Matson, P.A., Vitousek, P.M., Mooney, H.A., and Klooster, S.A. 1993. Terrestrial ecosystem production: a process model based on global satellite and surface data. *Global Biogeochem. Cycles*, **7**: 811–841.
- Potter, C.S., Davidson, E.A., and Verchot, L. 1996. Estimation of global biogeochemical controls and seasonality in soil methane consumption. *Chemosphere*, **32**: 2219–2246.
- Potter, C.S., Coughlan, J.C., and Brooks, V. 1999. Investigations of BOREAS spatial data in support of regional ecosystem modeling. *J. Geophys. Res.* **104**: 27 771 – 27 788.
- Potter, C.S., Wang, S., Nikolov, N.T., McGuire, A.D., Liu, J., King, A.W., Kimball, J.S., Grant, R.F., Frolking, S.E., Clein, J.S., Chen, J.M., and Amthor, J.S. 2001. Comparison of boreal ecosystem model sensitivity to variability in climate and forest site parameters. *J. Geophys. Res.* In press.
- Price, A.G., Dunham, K., Carleton, T., and Band, L. 1995. Water fluxes through the canopy and moss floor of a black spruce (*Picea mariana*) stand. *EOS*, **76**: 118.
- Priestly, C.H.B., and Taylor, R.J. 1972. On the assessment of surface heat flux and evaporation using large-scale parameters. *Mon. Weather Rev.* **100**: 81–92.
- Raich, J.W., and Potter, C.S. 1995. Global patterns of carbon dioxide emissions from soils. *Global Biogeochem. Cycles*, **9**: 23–36.
- Roulet, N.T., Ash, R., and Moore, T.R. 1992a. Low boreal wetlands as a source of atmospheric methane. *J. Geophys. Res.* **97**: 3739–3749.
- Roulet, N., Moore, T., Bubier, J., and Lafleur, P. 1992b. Northern fens: methane flux and climatic change. *Tellus*, **44B**: 100–105.
- Saugier, B., Granier, A., Pontailler, J.Y., Dufrene, E., and Baldocchi, D.D. 1997. Transpiration of a boreal pine forest measured by branch bag, sap flow, and micrometeorological methods. *Tree Physiol.* **17**: 511–519.
- Sellers, P., Hall, F., Margolis, J., Kelly, B., Baldocchi, D., den Hartog, G., Cihlar, J., Ryan, M.G., Goodison, B., Crill, P., Ranson, K.J., Lettenmaier, D., and Wickland, D.E. 1995. The Boreal Ecosystem–Atmosphere Study (BOREAS): an overview and early results from the 1994 field year. *Bull. Am. Meteorol. Soc.* **76**: 1549–1577.
- Shewchuk, S.R. 1997. The surface mesonet for BOREAS. *J. Geophys. Res.* **102**(D24): 29 077 – 29 082.
- Suyker, A.E., Verma, S.B., Clement, R.J., and Billesbach, D.P. 1996. Methane flux in a boreal fen: season-long measurement by eddy correlation. *J. Geophys. Res.* **101**: 28 637–28 647.
- Trofymow, J.A., Preston, C.M., and Prescott, C.E. 1995. Litter quality and its potential effect on decay rates of materials from Canadian boreal forests. *Water Air Soil Pollut.* **82**: 215–226.
- Trumbore, S., and Harden, J. 1997. Accumulation and turnover of carbon in organic and mineral soils of the BOREAS Northern Study Area. *J. Geophys. Res.* **102**(D24): 28 817 – 28 830.
- Trumbore, S.E., Bubier, J.L., Harden, J.W., and Crill, P.M. 1999. Carbon cycling in boreal wetlands: a comparison of three methods. *J. Geophys. Res.* **104**: 27 673 – 27 682.
- Veldhuis, H. 1998. BOREAS TE-20 NSA soil lab data. Available online at <<http://www.eosdis.ornl.gov/>> ORNL Distributed Active Archive Center, Oak Ridge National Laboratory, Oak Ridge, Tenn.
- Vitt, D., Bayley, S., Jin, T., Halsey, L., Parker, B., and Craik, R. 1990. Methane and carbon dioxide production from wetlands in boreal Alberta. Alberta Environment, Edmonton. Contract 90-0270.
- Windsor, J., Moore, T.R., and Roulet, N.T. 1992. Episodic fluxes of methane from subarctic fens. *Can. J. Soil Sci.* **72**: 441–452.
- Winston, G.C., Sunquist, E.T., Stephens, B.B., and Trumbore, S.E. 1997. Winter CO<sub>2</sub> fluxes in a boreal forest. *J. Geophys. Res.* **102**(D24): 28 795 – 28 804.
- Woodward, F.I. 1987. *Climate and plant distribution*. Cambridge University Press, Cambridge, U.K.
- Yin, X., and Arp, P.A. 1993. Predicting forest soil temperatures from monthly air temperature and precipitation records. *Can. J. For. Res.* **23**: 2521–2536.
- Zoltai, S.C., Taylor, S., Jeglum, J.K., Mills, G.F., and Johnson, J.D. 1988. Wetlands of boreal Canada. *In* *Wetlands of Canada*. National Wetlands Working Group, Environment Canada, Ottawa, Ont., and Polyscience Publications Inc., Montréal, Que. *Ecol. Land Classif. Ser.* 24. pp. 97–154.